energies

MDPI

Article

Optimization of Wind Energy Battery Storage Microgrid by Division Algorithm Considering Cumulative Exergy Demand for Power-Water Cogeneration

Mohammadali Kiehbadroudinezhad [1], Adel Merabet [1,*] and Homa Hosseinzadeh-Bandbafha [2]

[1] Division of Engineering, Saint Mary's University, Halifax, NS B3H 3C3, Canada; mohammadali.kiehbadroudinezhad@smu.ca
[2] Department of Mechanical Engineering of Agricultural Machinery, Faculty of Agricultural Engineering and Technology, University of Tehran, Karaj 77871-31587, Iran; homa.hosseinzadeh@ut.ac.ir
* Correspondence: adel.merabet@smu.ca; Tel.: +1-902-420-5712

Abstract: This study investigates the use of division algorithms to optimize the size of a desalination system integrated with a microgrid based on a wind turbine plant and the battery storage to supply freshwater based on cost, reliability, and energy losses. Cumulative exergy demand is used to identify and minimize the energy losses in the optimized system. Division algorithms are used to overcome the drawback of low convergence speed encountered by the well-known method genetic algorithm. The findings indicated that there is a positive relationship between cost, cumulative exergy, and reliability. More specifically, when the loss of power supply probability is 10%, compared to when it is 0%, the total cumulative exergy demand and total life cycle cost are reduced by 34.76% when the battery is full and 45.44% when the battery is empty and there is a 44.43% decrease in total life cycle cost, respectively. However, the more reliable system, the less exergy is lost during the production of 1 m^3 freshwater by desalination integrated into wind turbine plant.

Keywords: wind energy; cumulative exergy demand; reliability; optimization; division algorithm; desalination

Citation: Kiehbadroudinezhad, M.; Merabet, A.; Hosseinzadeh-Bandbafha, H. Optimization of Wind Energy Battery Storage Microgrid by Division Algorithm Considering Cumulative Exergy Demand for Power-Water Cogeneration. *Energies* **2021**, *14*, 3777. https://doi.org/10.3390/en14133777

Academic Editor: Djaffar Ould-Abdeslam

Received: 26 May 2021
Accepted: 18 June 2021
Published: 23 June 2021

1. Introduction

The 35% growth of the world population between 2015 and 2050 not only increases the demand for energy resources but also, leads to the rapid increase in the demand for freshwater [1]. Freshwater resources on Earth are limited, and to cope with the global freshwater demand, desalination is introduced as one of the most feasible solutions [2]. Among the various available technologies for desalination, reverse osmosis systems are recognized as economic technology [3]. However, reverse osmosis systems are energy-intensive; in better words, desalination of 1 m3 of freshwater approximately consumes 4 kWh of energy [4]. To address this challenge, the integration of desalination into renewable energy systems is suggested [5].

Despite all the favorable features of renewable energy, such as wind energy, renewable energy systems suffer from a time mismatch between power generation and consumption and subsequently low reliability [6]. The battery bank as a backup power can partly solve the problem [7]. However, consumption of non-renewable energy in battery bank manufacturing and even in the construction of renewable energy plants such as wind farms has caused broad concerns. Therefore, it is necessary to study the energy demand in the life cycle of electricity generation from wind-based systems including the total energy consumed in the manufacturing of system components, especially batteries.

Cumulative energy demand (CED) is one of the most important methodologies for studying and quantifying energy consumption according to a cradle to grave approach. It can calculate the total energy demand to produce a product or perform a process over its life cycle, from material extraction to waste management [8]. On the other hand, Bahlawan

et al. [9] reported a strong link between CED and critical environmental impacts such as abiotic resource depletion and global warming potential. However, it is based on the first law of thermodynamics; thus, its scientific robustness is not appropriate [10]. Also, it does not consider non-energetic materials and focus on the sources of the calorific value. In comparison, cumulative exergy demand (CExD) is based on thermodynamics' second law and includes non-energetic resources such as minerals and metal [10–12]. This indicator is introduced to depict the total exergy removal from nature to produce a product or perform a process [13]. Therefore, it could be a suitable indicator to study the energy in the life cycle of renewable energy systems.

On the other hand, high cost is the most significant barrier to renewable energy systems acceptance, as reported by Iskin et al. [14]. Although the cost of renewable energy-based systems has considerably reduced in recent years, they are still more expensive than fossil fuel-based systems [15]. Therefore, cost reduction is a crucial parameter for the successful adoption of renewable energy-based systems [16]. Various methods examine the costs in systems, life cycle cost (LCC) computes all production costs of a product with relatively high operating costs/long life span [17].

To have a reliable, low CExD, and cost-effective system based on renewable energy resources, it is required to optimize the size of the system. It should be noted that oversizing the system suffers from high initial costs, while its undersizing leads to energy shortfalls and operational limitations, despite lower initial costs [18]. Optimizing hybrid renewable energy systems reduces initial costs by energy storage and increases reliability due to various energy resources. The genetic algorithm (GA) as a population-based optimization method is widely used in hybrid renewable energy systems to obtain the optimal solution for a nonlinear optimization problem [19–23]. However, GA is easily trapped into local optimization [24]. Also, it has been reported that in solving real-world problems with complicated landscapes, GA suffers from low convergence speed [25]. For solving this problem, novel algorithms are proposed and developed to optimize the multi-objective problems. Recently, Kiehbadroudinezhad et al. [26] developed a novel algorithm named division algorithm (DA) to optimize reliable and cost-effective desalination based on renewable energy resources. They claimed that in solving problems, DA is flexible, simple, precise, and fast compared to GA.

Generally, islands and higher altitude zones that are usually far from freshwater sources and close to the seawater have a high potential to use wind energy to produce fresh water from the desalination process [27]. Due to this fact, the present study proposes using wind energy to generate the electricity required in the desalination process to supply freshwater to the inhabitants of Larak Island, Iran. Nevertheless, as mentioned, optimal sizing of systems based on renewable energy can lead to increased cost-effectiveness and reliability as well as exergy management. Accordingly, this paper searches for the best system size based on cost, reliability, and exergy demand which has been neglected so far.

Although various studies design, model, and optimize desalination integrated with renewable energy in terms of size, reliability, and cost, but the CExD of systems is not still widely discussed. This paper has provided a deeper insight into the role of optimal size and reliability on the exergy flow of desalination. In better words, this paper contributes to existing knowledge of wind energy battery storage microgrid by providing a new algorithm, that is, DA, and a new objective function, that is, minimum CExD. The findings reported here contribute to a better understanding of exergy flow in renewable energy systems and provide a basis for paying attention to optimizing the exergy flow in renewable energy systems. The findings from this study also contribute to understanding the relationship between exergy flow and reliability in renewable energy systems.

To achieve the purpose, the first section of this paper explains the modeling of desalination integrated with a renewable energy system. The second section focuses on cost modeling, followed by modeling cumulative exergy demand and cumulative degree of perfection (CDP). The third section describes system reliability followed by *the power control*

system. The fourth section explains the problem of optimization and the proposed algorithm. Finally, in the fifth section, the optimization results will be presented and discussed.

2. Materials and Methods

2.1. Modeling of Wind Turbine (WT)

Wind is introduced as the most mature and cost-efficient renewable resource for electricity generation among different renewable resources [28–30]. A wind turbine converts the mechanical energy of wind into electrical energy [31]. Generally, two influential parameters play a critical role in the amount of power output of WT, that is, wind speed and height of the WT hub that could be modeled using Equation (1) [26]:

$$\frac{V}{V_0} = \left[\frac{h}{h_0}\right]^{\alpha} \tag{1}$$

In this equation, α denotes the power-law exponent, and V and V_0 are wind speeds at height h and h_0 or reference height. Moreover, the power output of WT could be modeled as follows [7]:

$$P_{WT} = \begin{cases} 0, \ V(t) \le Vci \ or \ V(t) \ge Vco \\ a \times V^3 - b \times P_r, \ Vci \le V(t) \le Vr \\ P_r, \quad Vr \le V(t) \le Vco \end{cases} \tag{2}$$

$$a = \frac{P_r}{\left({V_r}^3 - V_{ci}\right)} \tag{3}$$

$$b = \frac{{V_{ci}}^3}{\left({V_r}^3 - {V_{ci}}^3\right)} \tag{4}$$

where P_{WT} and P_r are power output from WT and rated power of a WT, respectively. Also, V_{ci}, V_{co}, and V_r represent cut-in wind speed, cut-out wind speed, and rated WT speed, respectively. When the number of WT (N_{WT}) is more than 1, the power output of WTs (P_T) is obtained using Equation (5):

$$P_T = N_{WT} \times P_{WT} \tag{5}$$

Moreover, P_r could be modeled using Equation (6):

$$P_r = 1/2 \times A_{WT} \times C_p \times \rho_a \times \eta_r \times \eta_{WT} \times {V_r}^3 \tag{6}$$

In this equation, A_{WT} is the area swept by WT's blades, η_{WT} *is* WT efficiency, η_r *is* reducer efficiency, ρ_a is the air density, and C_p is the power coefficient.

2.2. Modeling of Battery Bank Storage (BBS)

As mentioned, batteries are commonly used in systems based on renewable energy to achieve higher reliability. When the desalination plant's power demand is less than the power generated by WT, BBS acts as a power storage unit that the capacity of the BBS in this mode could be calculated using Equation (7) [32]:

$$SOC(t) = SOC(t-1) \times (1-\sigma) + \left[P_{WT}(t) - \frac{P_L(t)}{\eta_{Inv}}\right] \times \eta_{BC} \tag{7}$$

where *SOC(t)* is the BBS charge at time t ($SOC_{min} \ge SOC(t) \ge SOC_{max}$) and $SOC(t-1)$ denotes the BBS charge at time $t-1$. Also, P_L is the desalination plant's power demand, σ represents the hourly self-discharge rate, η_{Inv} shows charge efficiency of inverter efficiency, and η_{BC} indicates charge efficiency of BBS.

On the other hand, when the desalination plant's power demand is more than the power generated by WT, BBS acts as power support units that the available BBS capacity in this mode, that is, discharging mode, could be calculated using Equation (8):

$$SOC(t) = SOC(t-1) \times (1-\sigma) - \left[\frac{P_L(t)}{\eta_{Inv}} - P_{WT}(t)\right] / \eta_{BF} \quad (8)$$

where η_{BF} denotes the discharge efficiency of the BBS. It should be noted that loss of power supply (LPS) could also be estimated by Equation (9):

$$\mathrm{LPS}(t) = \frac{P_L(t)}{\eta_{Inv}} - P_{WT}(t) - [SOC(t-1) \times (1-\sigma) - SOC_{\min}(t)] \times \eta_{BF} \quad (9)$$

2.3. Modeling of Seawater Reverse Osmosis Desalination (SWROD)

Power consumption per hour in a desalination plant depends on the volume of hourly freshwater demand that is obtained as follows:

$$P_{DEM} = H_{WD} \times S_{DC} \quad (10)$$

P_{DEM} is the hourly power consumption of the desalination plant, H_{WD} is the hourly water demand, and S_{DC} is the specific energy consumption of the desalination plant. In the current study, the power required by the desalination plant is determined by ROSA software. This software could also assess the desalination plant's specific energy consumption, freshwater and seawater quality, membrane type, flow permeate rate, and structure and pressure of the vessels [26]. In this study, the daily water capacity that desalination could generate is estimated as follows [33]:

$$D_{WC} = 24 \times \left(\frac{P_D}{S_{DC}}\right) \quad (11)$$

In this equation, D_{WC} and P_D are daily water capacity and desalination installed power, respectively. Overall, P_D is between minimum power (P_{MD}) and nominal power (P_{DI}) [34]. Notably, the excess freshwater produced by the desalination plant is stored in the water tank (WTa). If the freshwater is kept for two days, the water tank capacity is obtained as follows:

$$V_{WTa} = 2 \times D_{WD} \quad (12)$$

V_{WTa} is the water tank's capacity, and D_{WD} is the total capacity pertaining to the daily freshwater demand.

2.4. Economic Modeling

LCC_{WT} or total life cycle cost of *WT* includes total investment cost (CC_{WT}) and the maintenance cost (MC_{WT}) of WT that could be modeled as follows:

$$LCC_{WT} = CC_{WT} + MC_{WT} \quad (13)$$

In this equation, CC_{WT} and MC_{WT} are obtained using Equations (14) and (15), respectively:

$$CC_{WT} = A_{WT} \times C_{WT} \times CRF \quad (14)$$

$$MC_{WT} = C_{Mnt\text{-}WT} \times A_{WT} \times \sum_{k=0}^{19} \frac{1}{(1+i)^k} \times CRF \quad (15)$$

C_{WT} is the WT price and the WT installation fee, $CM_{nt\text{-}WT}$ is the maintenance cost of each WT per year, and *CRF* is the capital recovery coefficient which is defined as follows:

$$CRF(i,n) = \frac{i(1+i)^n}{(1+i)^n - 1} \quad (16)$$

In this equation, I indicates the system's interest rate, and n denotes the system's life span.

LCC of BBS also is the sum of the investment cost of BBS (CC_{BBS}) and maintenance and operation cost of BBS (MC_{BBS}) that could be calculated Equations (17) and (18), respectively:

$$CC_{BBS} = N_{BBS} \times PW_{BBS} \times CRF \tag{17}$$

$$MC_{BBS} = N_{BBS} \times C_{Mnt-BBS} \tag{18}$$

N_{BBS} is the number of battery banks, $CM_{nt\text{-}BBS}$ is the maintenance cost of each BBS in a year, and PW_{BBS} is payment present worth factor of battery that could be obtained as:

$$PW_{BBS} = C_{BBS} \times \sum_{k=0,5,10,15} \frac{1}{(1+i)^k} \tag{19}$$

where C_{BBS} is battery cost. Notably, in this study, the battery bank lifetime is assumed five years.

Also, alternating current is converted to direct current by converter/inverter that its LCC of converter/inverter could be determined as follows:

$$LCC_{Conv/Inv} = CC_{Conv/Inv} + MC_{Conv/Inv} \tag{20}$$

where $CC_{Conv/Inv}$ is the investment cost of the electric current converter and could be expressed as follows:

$$CC_{Conv/inv} = N_{Conv/Inv} \times PW_{Conv/Inv} \times CRF \tag{21}$$

where $NC_{onv/Inv}$ is the number of converters, and $PW_{Con/Inv}$ is the payment present worth factor of converter/inverter as follows:

$$PW_{Conv/inv} = C_{Conv/Inv} \times \sum_{k=0,10} \frac{1}{(1+i)^k} \tag{22}$$

$MC_{Conv/Inv}$, that is, the maintenance cost of the electric current converter, is modeled using Equation (23):

$$MC_{Conv/Inv} = N_{Conv/Inv} \times C_{Mnt-Conv/Inv} \tag{23}$$

$C_{Mnt\text{-}Conv/Inv}$ is the maintenance cost of the converter per year.

Finally, LCC of SWROD is the sum of the investment cost of SWROD (CC_{SWROD}), the maintenance cost of SWROD (MC_{SWROD}), membrane replacement cost (TC_{MR}), water tank cost (CC_{WTa}), and the chemical cost (TC_{CH}) that could be computed using Equations (24)–(28), respectively:

$$\mathrm{CC_{SWROD}} = C_{\mathrm{SWROD}} \times \mathrm{Ca_{WD}} \times CRF \tag{24}$$

$$\mathrm{MC_{SWROD}} = C_{\mathrm{Mnt-SWROD}} \times D_{\mathrm{WD}} \tag{25}$$

$$TC_{\mathrm{MR}} = C_{\mathrm{MR}} \times \mathrm{Ca_{WD}} \times N_{Me} \tag{26}$$

$$\mathrm{CC_{WTa}} = C_{\mathrm{WTa}} \times V_{\mathrm{WTa}} \times CRF \tag{27}$$

$$TC_{\mathrm{CH}} = C_{\mathrm{CH}} \times D_{\mathrm{WD}} \tag{28}$$

In Equation (24), C_{SWROD} and Ca_{wd} are the cost of the SWROD plant and the capacity of the desalination plant per day, respectively. In Equation (25), $C_{Mnt\text{-}SWROD}$ is the maintenance cost of SWROD per year and D_{WD} is the total freshwater demand per day. In Equation (26), C_{MR} and N_{Me} are the cost of membrane replacement and the number of membrane replacements per year, respectively. In Equation (27), C_{WTa} is the sum of the price to buy and install the water tank, and V_{WTa} is the volumetric capacity of the water tank. Finally, in Equation (28), C_{CH} is the cost of chemicals used in desalination.

2.5. Modeling Cumulative Exergy Demand (CExD)

To find an optimized model in hybrid energy systems, identifying and minimizing the energy losses is essential. However, conventional energy analysis, which relies on the first law of thermodynamics, cannot consider the quality of energy inputs and energy losses [35]. Therefore, the exergy analysis based on the second law of thermodynamics has been developed to meet this challenge, as previously mentioned. The CExD indicates the sum of exergy of all the natural resources used to produce a product during the life cycle, that is, the cradle to grave approach, that could be determined by the natural resources' exergy values [36]. To calculate the CExD, first, inventory data were collected from all energy and materials used in freshwater production by developed configuration in the current study, that is, seawater reverse osmosis desalination/wind turbine/battery bank storage (SWROD/WT/BBS) (Figure 1). Data related to energy carriers and materials used in producing components in the system named (background data) were extracted from EcoInvent database [37]. Data related to chemical consumption for membrane cleaning and other chemicals were not included in the analysis. It should be noted that energy form categories of CExD include "non-renewable, fossil", "non-renewable, nuclear","non-renewable, primary", "non-renewable, minerals", "non-renewable, metals," "renewable, kinetic", "renewable, potential", "renewable, solar", "renewable, biomass" and "renewable, water". In the current research, CExD was calculated for 1 m^3 as the functional unit (FU).

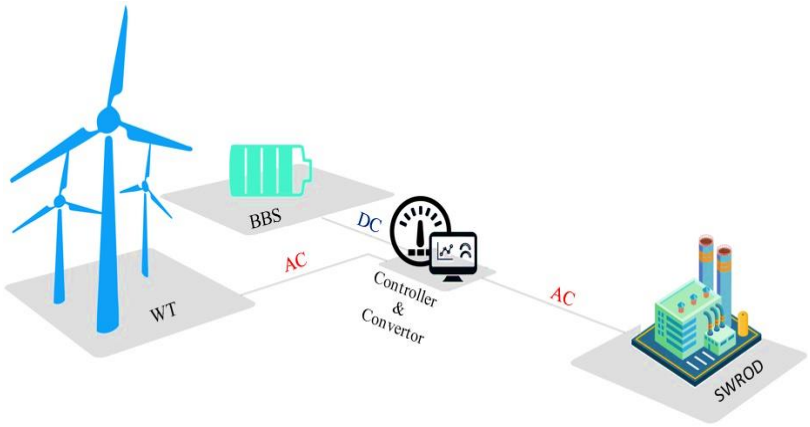

Figure 1. Developed configurations for freshwater production in the current study.

In addition, CDP was obtained for comparative exergy analysis of freshwater production by developed configuration. CDP is defined as the ratio of the exergy content of the final product (electricity generated) to the total CExD of the final product [38]. It should be noted that a higher CDP implies better savings and more efficient consumption of inputs in the system. It should be noted that results are provided both for when the batteries are fully charged and for when the batteries are charged using a turbine.

2.6. Modeling the System Reliability

The power required for desalination should be uninterruptedly provided by a reliable power generating system. Loss of power supply probability (LPSP) is introduced as a critical parameter to determine the reliability of a power-generating system [39]. Generally, LPSP that could be calculated by Equation (29) varies from zero to one; when it is zero, the power requirement can be satisfied, and when it is one, it cannot be satisfied [40,41].

$$LPSP(t) = \frac{\sum_{t=1}^{T} LPS(t)}{\sum_{t=1}^{T} P_L(t)} \quad (29)$$

2.7. Power Control System

In this study, a power control system is designed according to the relationship between the power demand of desalination and power generated by WT (Figure 2). When the power demand of desalination and power generated by WT are the same, all the power generated is directed to desalination, and no power is stored in the BBS (Equation (30)).

$$P_{WT} = P_{Load} \tag{30}$$

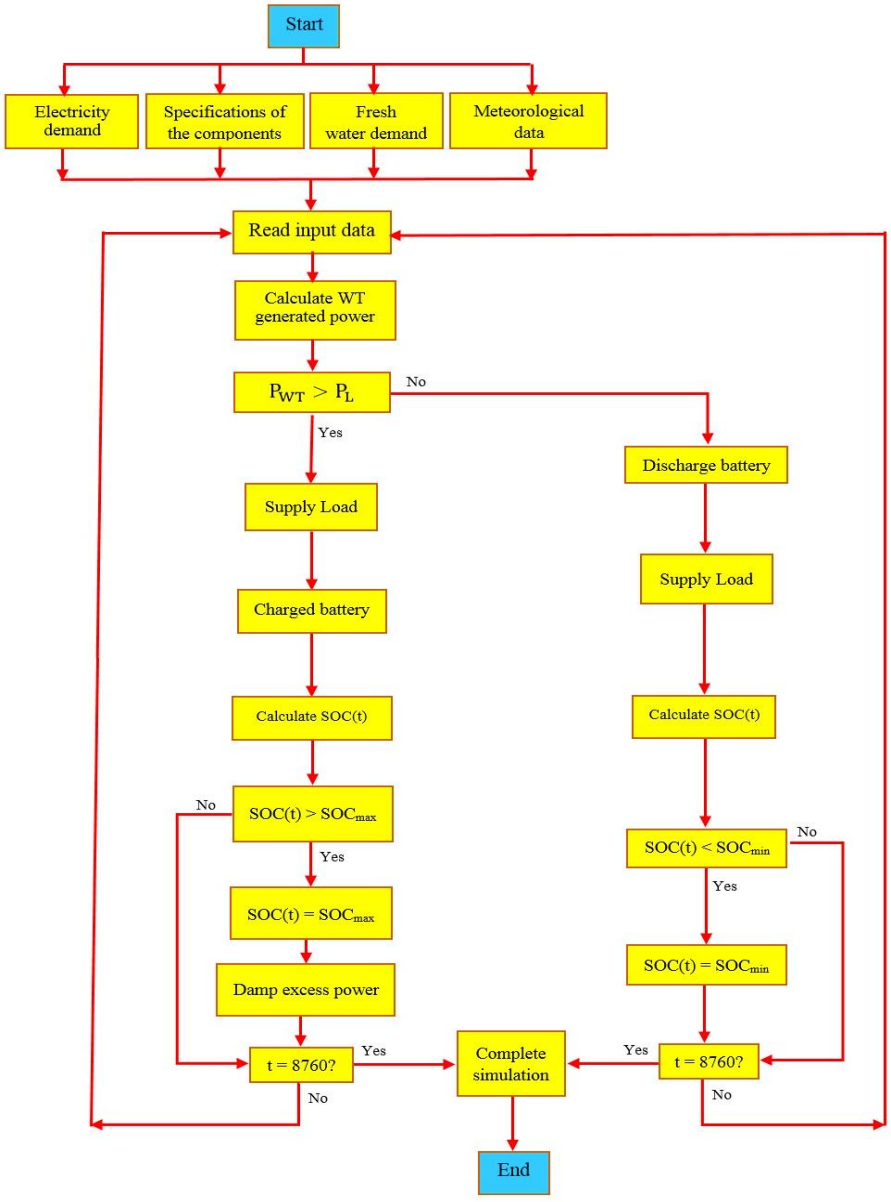

Figure 2. Flowchart of the power control and management for power system considered. Adapted from [26]. With permission from Wiley. Copyright© 2021; License Number: 5076070232025.

On the other hand, when the power demand of desalination is more than the power generated by WT, the power required could be supplied using BBS (Equation (31)).

$$P_{WT} < P_{Load} \tag{31}$$

Finally, when power the demand of the desalination is lower than the power generated by WT, the surplus power could be stored in BBS. The remaining surplus power could also be directed out of the system by the damper (Equation (32)).

$$P_{WT} > P_{Load} \tag{32}$$

2.8. Optimization Problem

Typically, the objective function is defined based on one or more continuous and/or discrete decision variables that the values of these variables are determined by the optimization models [42]. For optimizing the size of the system, two decision variables are considered in the current study, that is, A_{WT} as a continuous decision variable and N_{BBS} as a discrete decision variable.

According to optimization objectives, the objective function could be defined using Equation (33):

$$Minimize\ TLCC\ (\ A_{WT},\ N_{BBS}) = Min.\ \sum_{m=WT,BBS,Conv/Inv,SWROD} TLCC_m \tag{33}$$

There are constraints in solving the optimization problem of this study that are listed in Equations (34)–(39):

$$A_{WT} \geq 0 \tag{34}$$

$$N_{BBS} \geq 0 \tag{35}$$

$$LPSP^m \geq LPSP \tag{36}$$

$$SOC_{min} \leq\ SOC(t)\ \leq\ SOC_{max} \tag{37}$$

$$SOC_{min} = (1\text{–}DOD) \times S_{BBS} \tag{38}$$

$$P_{WT}(t) + P_{BBS}(t) \geq\ P_L(t) \tag{39}$$

$LPSP^m$ is the maximum $LPSP$, and S_{BBS} and DOD represent nominal battery bank capacity and the battery bank's depth of discharge, respectively.

As previously mentioned, this study follows the DA, which is faster, simpler, more flexible, and precise than the GA for optimization, since it overcomes the disadvantages of GA [26,43]. For example, the DA could work without operators like crossover and mutation and reduce the complexity. The implementation process of the DA for the current study coded by MATLAB software is demonstrated in Figure 3.

2.9. Characteristics of Case Study

The design of a renewable energy-based desalination plant in Larak Island, Iran is presented as a goal. Larak Island (Longitude: 56°21′20.0″ E and Latitude: 26°51′12.0″ N) with an area of about 49 km^2 is an island off the coast of Iran (Figure 4). The drinking water of the island's households, estimated at 261 households, is mainly provided by Bandar Abbas, Iran. This dependence leads to difficulties in access to freshwater for the inhabitants of this island. Nevertheless, this island is surrounded by the sea; thus, launching a desalination plant could be a promising option for non-dependence on other areas in the water supply. On the other hand, according to data extracted from NASA (https://power.larc.nasa.gov/ accessed on 12 January 2020), there is a high potential for using wind as a renewable energy resource.

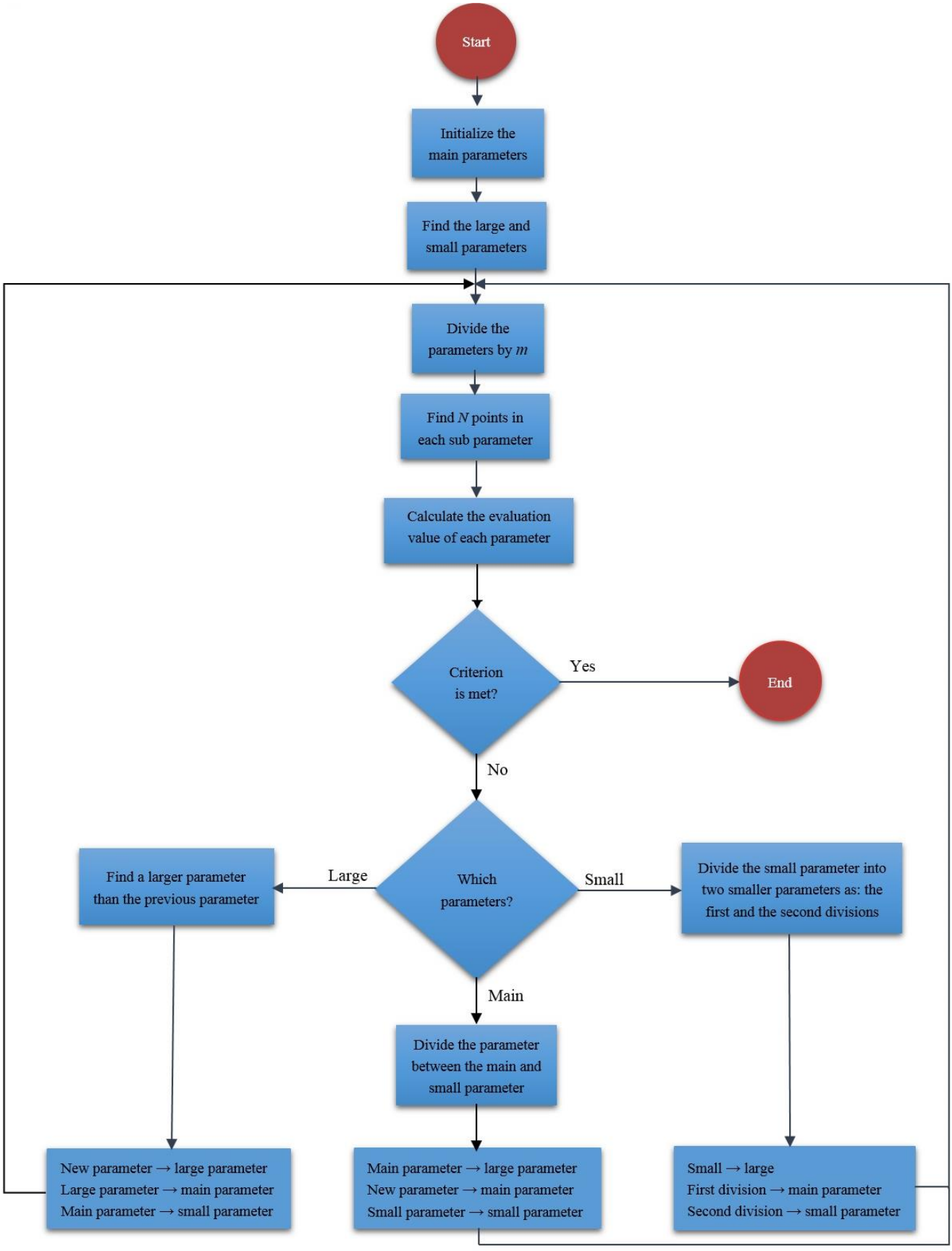

Figure 3. The implementation process of the division algorithm used in the current study [26]. With permission from Wiley. Copyright© 2021; License Number: 5076070602065.

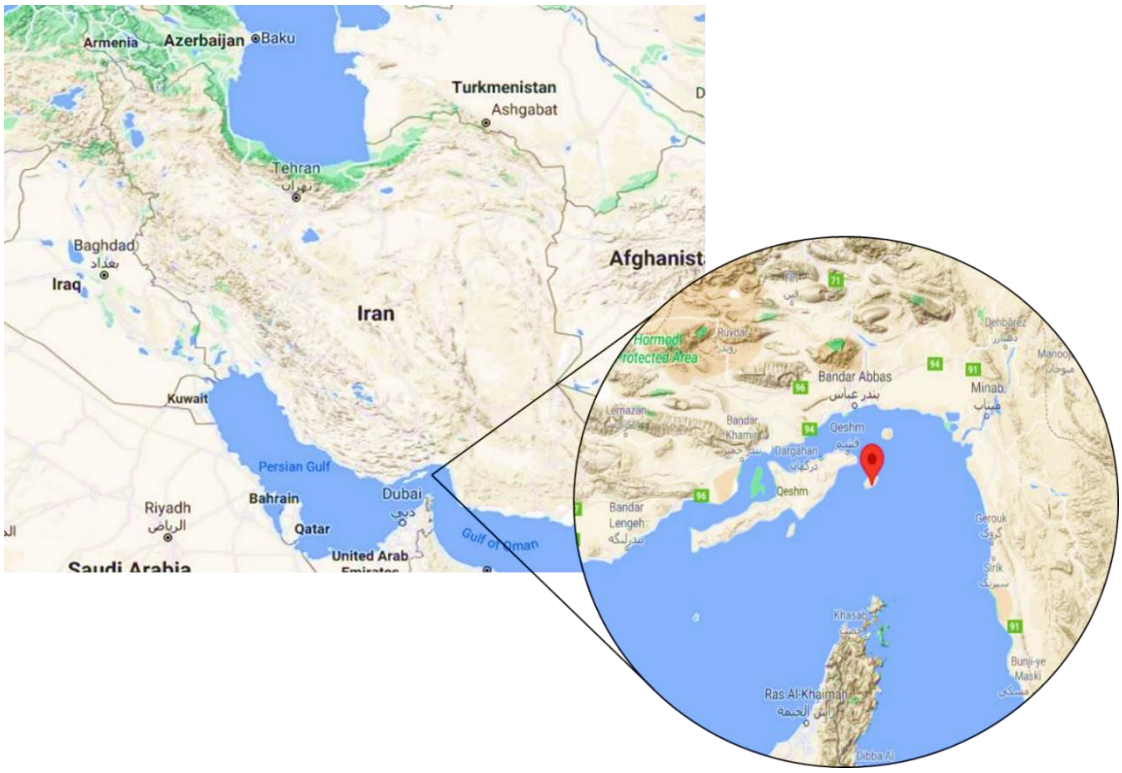

Figure 4. Location of Larak Island in the south of Iran [google maps].

3. Results and Discussion

According to the objective function and the DA, the size of the components of desalination based on wind energy are optimized, and the results are summarized in Table 1. Findings illustrate that there is an inverse relationship between LPSP and LCC and CExD for producing 1 m^3 of freshwater. More specifically, when LPSP is 10%, compared to LPSP is 0%, the total CExD is reduced by 34.76% and 45.44%, for when the battery is full and empty, respectively. Also, there is a 44.43% decrease in the total LCC of 1 m^3 of freshwater. In our previous study [26], which focused on costs and reliability, cost optimization results were well discussed. This study focuses on CExD for producing 1 m^3 of freshwater, which is discussed in more detail below.

Table 1. LCC and CExD or producing 1 m^3 of freshwater according to the optimal size of system components. Data associated with the size of system components extracted from [26].

SWROD	AWT (m^2)	N_{BBS}	LPSP (%)	LCC ($/$m^3$)	CExD (MJ/m^3) [A]	CExD (MJ/m^3) [B]
1	104.6	117	0	38.10	12.80	18.21
1	92.1	110	2	33.33	11.50	16.61
1	78.8	101	5	29.03	10.10	14.80
1	61.5	90	10	21.17	8.35	12.52

[A] When the battery is full. [B] When the battery is empty.

Although the energy consumed in desalination is wind and does not have concerns associated with non-renewable energy, one should not ignore the energy consumption in the manufacturing process of components. Knowledge of the type and amount of energy consumption in the life cycle of producing 1 m^3 of freshwater by desalination integrated to WT helps better manage energy consumption. The results presented in Table 2 show the type and amount of energy consumption for producing 1 m^3 freshwater in terms of CExD when the battery is full. The results indicate that exergy removal from nature in freshwater production by SWROD/WT/BBS is primarily in the form of "renewable, kinetic" in the

range of 5.56–9.46 MJ/FU and followed by "non-renewable, fossil" in the range of 1.8–2.17 MJ/FU. Other impacts categories have less of a contribution in the total amount of exergy removal from nature. The contribution of impact categories in developing the total CExD for producing 1 m^3 freshwater are presented in Figure 5, for LPSP it is 0%, 2%, 5%, and 10%.

Table 2. CExD for producing 1 m^3 freshwater by SWROD/WT/BBS in various impact categories when the battery is full.

Impact Category	Unit	LPSP (%)			
		0	2	5	10
Total	MJ	1.28 E + 01	1.15 E + 01	1.01 E + 01	8.35 E + 00
Non-renewable, fossil	MJ	2.17 E + 00	2.07 E + 00	1.95 E + 00	1.80 E + 00
Non-renewable, nuclear	MJ	2.17 E − 01	2.05 E − 01	1.91 E − 01	1.74 E − 01
Renewable, kinetic	MJ	9.46 E + 00	8.33 E + 00	7.12 E + 00	5.56 E + 00
Renewable, solar	MJ	4.30 E − 05	3.99 E − 05	3.61 E − 05	3.15 E − 05
Renewable, potential	MJ	9.88 E − 02	9.22 E − 02	8.42 E − 02	7.43 E − 02
Non-renewable, primary	MJ	1.71 E − 04	1.61 E − 04	1.48 E − 04	1.31 E − 04
Renewable, biomass	MJ	5.51 E − 02	5.15 E − 02	4.71 E − 02	4.16 E − 02
Renewable, water	MJ	5.94 E − 02	5.58 E − 02	5.13 E − 02	4.58 E − 02
Non-renewable, metals	MJ	7.30 E − 01	7.09 E − 01	6.83 E − 01	6.52 E − 01
Non-renewable, minerals	MJ	1.35 E − 02	1.24 E − 02	1.11 E − 02	9.51 E − 03

Table 3, also shows the type and amount of energy consumption for producing 1 m^3 freshwater in terms of CExD when the battery is empty and energy must be supplied by turbines. In addition, the contribution of impact categories in developing the total CExD in this mode, for producing 1 m^3 freshwater are presented in Figure 6, for LPSP is 0%, 2%, 5%, and 10%. Due to the consumption of wind energy to charge the batteries, the share of this energy is increased compared to when the batteries are fully charged.

Table 3. CExD for producing 1 m^3 freshwater by SWROD/WT/BBS in various impact categories when the battery is empty.

Impact Category	Unit	LPSP (%)			
		0	2	5	10
Total	MJ	1.82 E + 01	1.66 E + 01	1.48 E + 01	1.25 E + 01
Non-renewable, fossil	MJ	2.41 E + 00	2.29 E + 00	2.15 E + 00	1.98 E + 00
Non-renewable, nuclear	MJ	2.40 E − 01	2.27 E − 01	2.11 E − 01	1.91 E − 01
Renewable, kinetic	MJ	1.45 E + 01	1.31 E + 01	1.15 E + 01	9.48 E + 00
Renewable, solar	MJ	4.83 E − 05	4.49 E − 05	4.07 E − 05	3.56 E − 05
Renewable, potential	MJ	1.10 E − 01	1.03 E − 01	9.42 E − 02	8.32 E − 02
Non-renewable, primary	MJ	1.82 E − 04	1.71 E − 04	1.57 E − 04	1.40 E − 04
Renewable, biomass	MJ	6.16 E − 02	5.76 E − 02	5.27 E − 02	4.66 E − 02
Renewable, water	MJ	6.36 E − 02	5.97 E − 02	5.49 E − 02	4.90 E − 02
Non-renewable, metals	MJ	7.71 E − 01	7.48 E − 01	7.19 E − 01	6.84 E − 01
Non-renewable, minerals	MJ	1.63 E − 02	1.51 E − 02	1.36 E − 02	1.17 E − 02

As shown, when system reliability is reduced, a decrease in the contribution of "renewable, kinetic" or wind energy is recorded. In contrast, an increase is shown in the contribution of "non-renewable, fossil." Therefore, it can be concluded that the lower the system's reliability, the greater the share of "non-renewable, fossil" in the system. Given the adverse consequences of non-renewable energy, finding its source in the current study is essential. Figure 7 demonstrates the contribution of various system components in producing 1 m^3 freshwater by SWROD/WT/BBS for the "non-renewable, fossil" impact category based on different LPSP (%) when the battery is full (Figure 7A) and when the battery empty (Figure 7B).

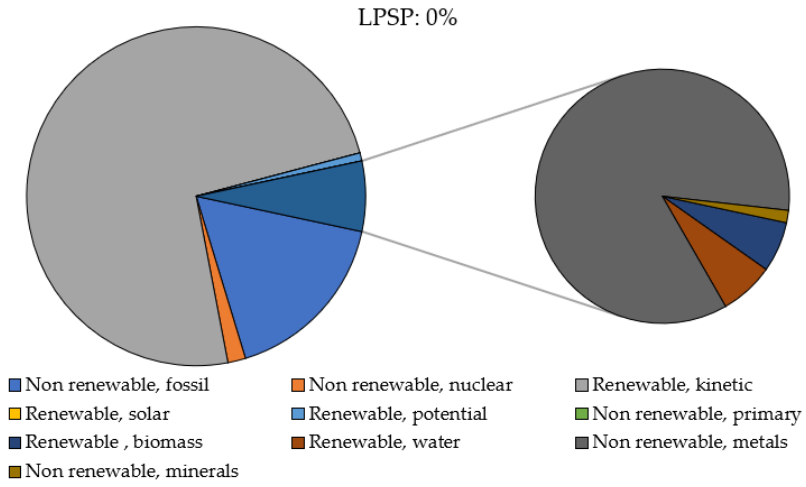

(**a**)

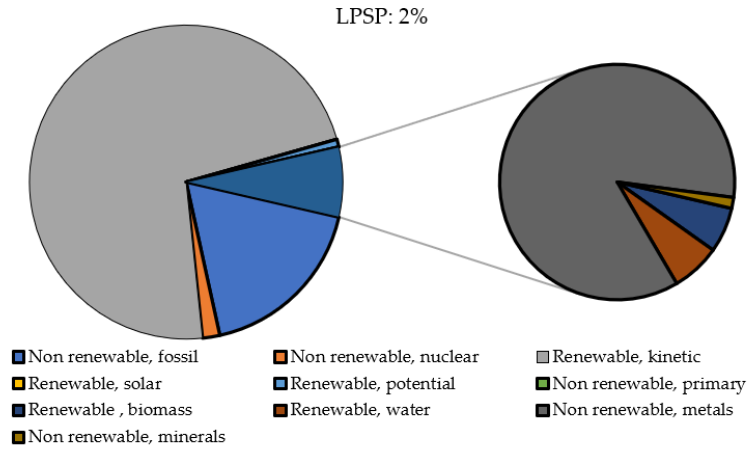

(**b**)

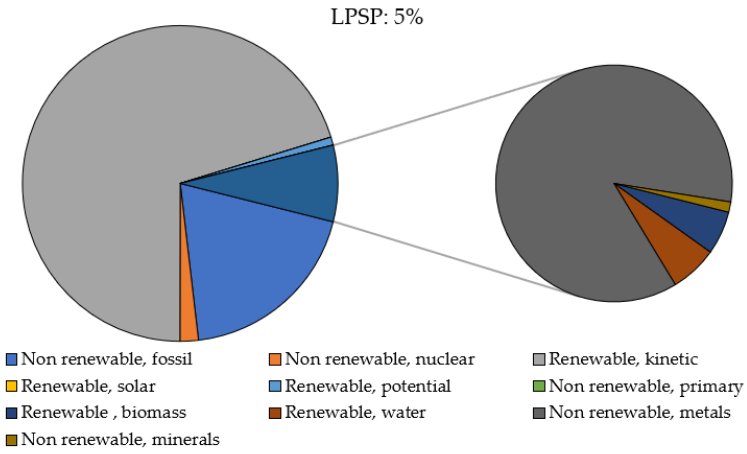

(**c**)

Figure 5. *Cont.*

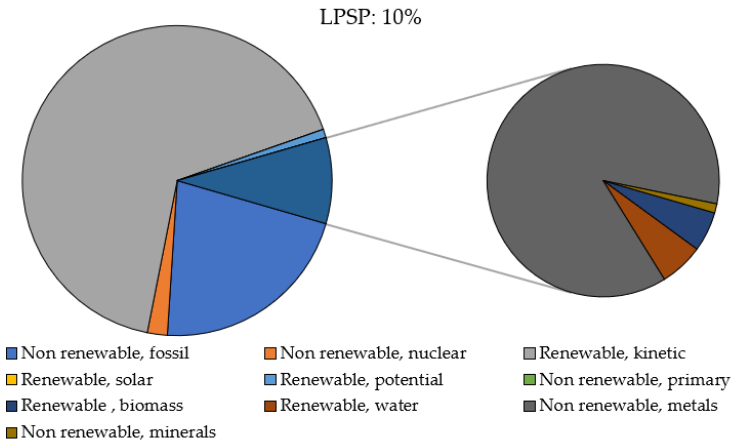

(**d**)

Figure 5. The contribution of impacts categories in developing the total CExD for producing 1 m^3 freshwater by SWROD/WT/BBS when the battery is full. (**a**) LPSP 0%, (**b**) LPSP 2%, (**c**) LPSP 5%, and (**d**) LPSP 10%.

The water tank (polyethylene) exhibited the highest effect on the "non-renewable, fossil" impact category, followed by battery for all different LPSP (%). Fossil fuels often produce polyethylene. More specifically, ethylene gas is the main ingredient for polyethylene made from crude oil and natural gas [44]. Thathiana Benavides et al. [44] reported that feedstock production, that is, natural gas and crude oil, is the most significant contributor to the consumption of fossil fuels in polyethylene production. Although the recycling of waste polyethylene is widely regarded as a cost-effective and eco-friendly technology [45], appropriate approaches should be considered that reduce the use of polyethylene. Because the recycling process, in turn, leads to the consumption of fossil fuels, Thathiana Benavides et al. [44] suggested bio-polyethylene production instead of fossil-polyethylene production. They reported that bio-polyethylene production leads to a reduction of 63% in fossil fuel consumption. In addition to reducing fossil fuel consumption, bio-polyethylene leads to decreased carbon dioxide emissions [44,46,47]. However, in comparison with fossil-based plastics, bio-based plastics with similar mechanical properties are expensive [48]. Therefore, future research is recommended on the production of bio-polyethylene at competitive prices with polyethylene.

Inventory analysis shows that graphite used in battery production has a significant role in the "non-renewable, fossil" impact category. According to Notter et al. [49], graphite is made from hard coal coke as base material; thus, hard coal used in graphite production is main responsible for the "non-renewable, fossil" impact category. Given that the presence of a battery is essential to increase the system's reliability, its presence is necessary; therefore, it should be directed towards the production of batteries that consume fewer fossil fuels. For example, Padashbarmchi et al. [50] claimed that metal oxides such as iron oxide, more than graphite, are favorable anode materials in fossil fuel consumption. Due to the higher operation of the power plant to supply the battery charge, the plant's share will increase when the battery is empty.

Figure 8 presents the CDP values in the production of 1 m3 freshwater by SWROD/WT/BBS. In Figure 8, there is a clear trend of decreasing CDP with increasing LPSP. The higher value of CDP indicates that lower exergy is lost, that is, the exergy performance of the system is higher in the production process [51]. Accordingly, it could be said that the more reliable the system, the less exergy is lost during the production of 1 m3 freshwater by SWROD/WT/BBS. To improve CDP, strategies can be used to reduce CExD, especially the "non-renewable, fossil" impact category, as previously described. On the other hand, more efficient desalination plants should be designed to consume less electricity to produce fresh water.

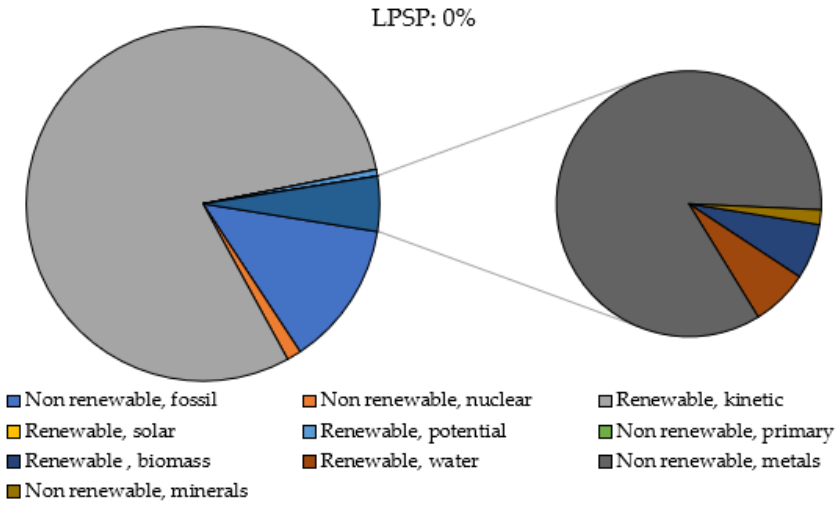

(**a**)

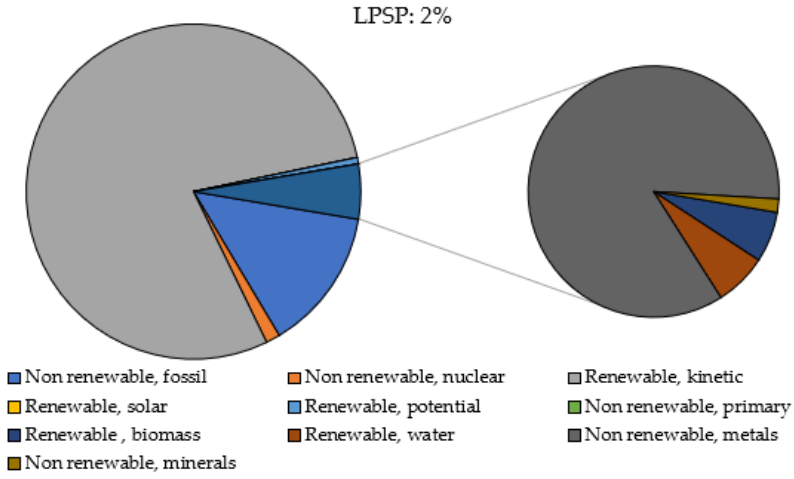

(**b**)

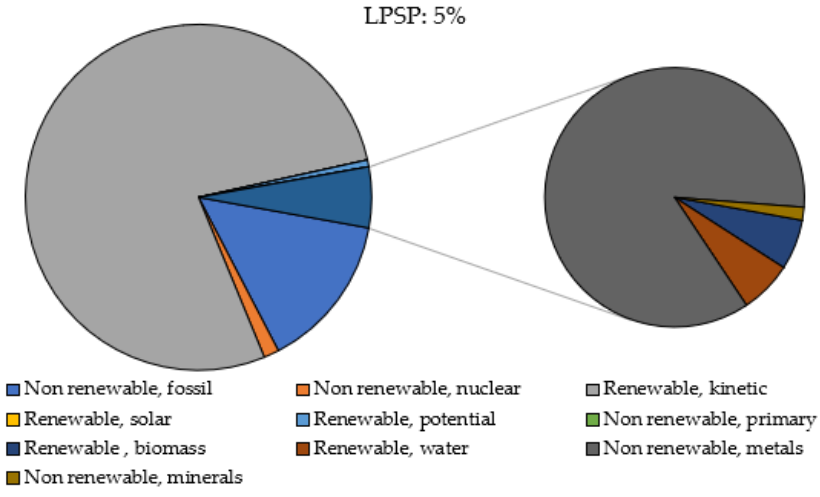

(**c**)

Figure 6. *Cont.*

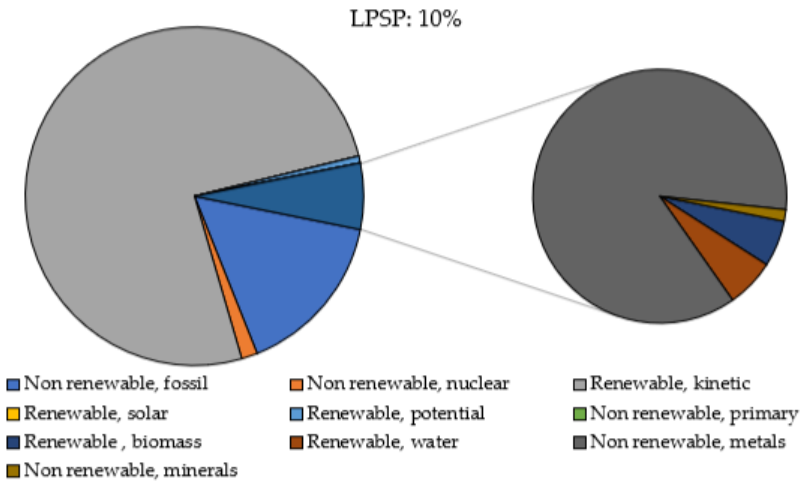

(**d**)

Figure 6. The contribution of impacts categories in developing the total CExD for producing 1 m^3 freshwater by SWROD/WT/BBS when the battery is empty. (**a**) LPSP 0%, (**b**) LPSP 2%, (**c**) LPSP 5%, and (**d**) LPSP 10%.

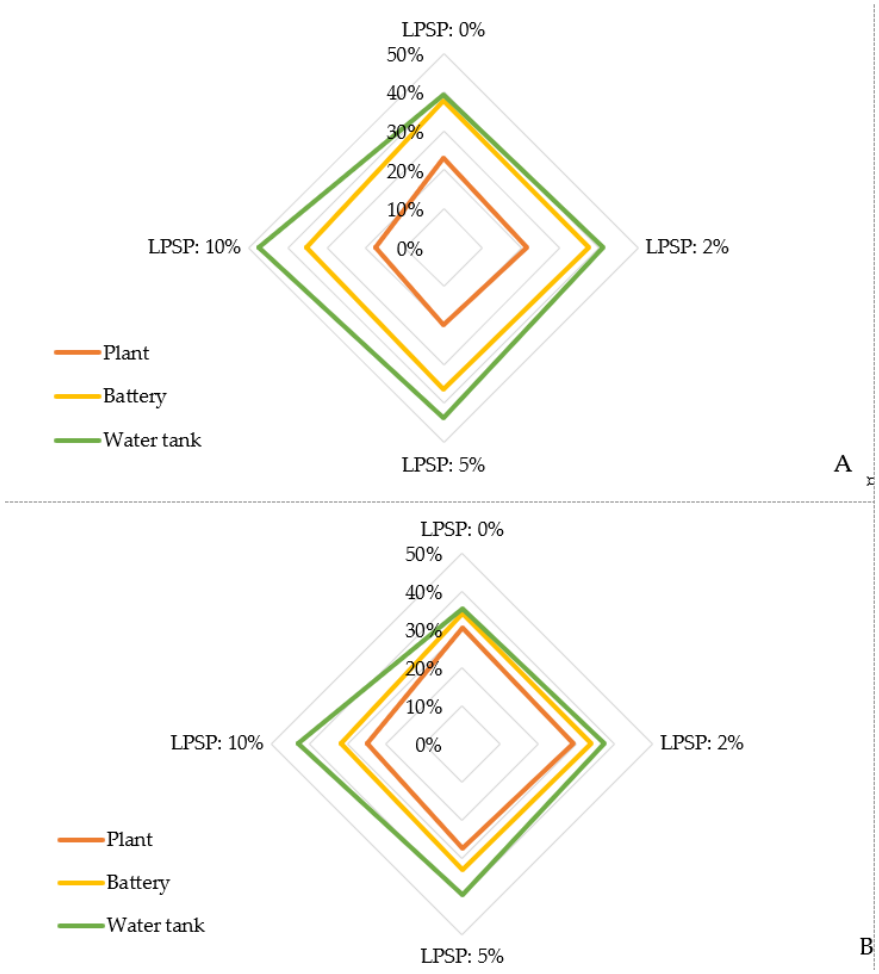

Figure 7. Contribution of various components of the system in the production of freshwater by SWROD/WT/BBS for "non-renewable, fossil" impact category based on different LPSP (%) (FU = 1 m^3). (**A**) when the battery is full and (**B**) when the battery is empty.

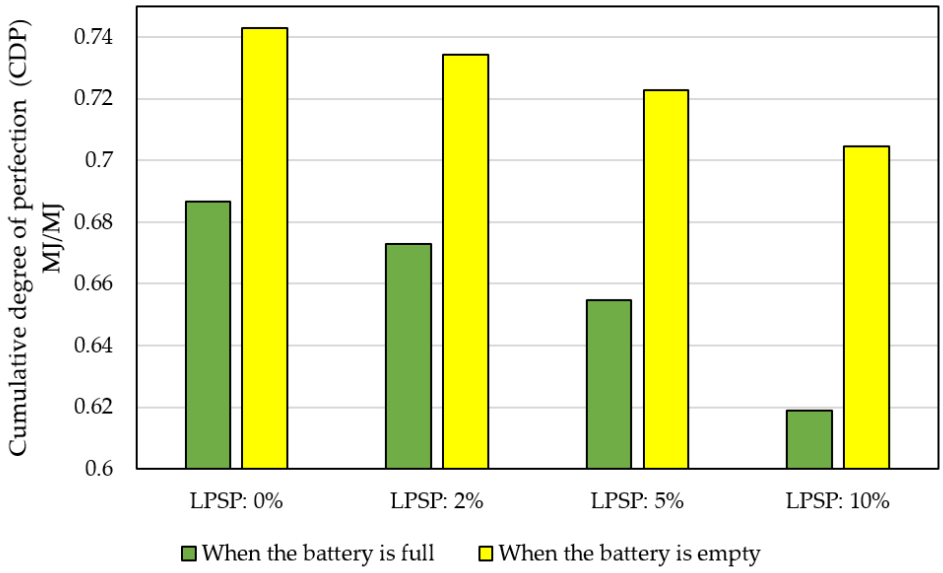

Figure 8. Cumulative degree of perfection in freshwater production by SWROD/WT/BBS based on different LPSP (%) (FU = 1 m^3).

Finally, Figure 9 shows the convergence speed to reach the optimal solution for the DA optimization algorithms compared to GA and the artificial bee swarm optimization (ABSO) algorithms. Based on the results, the DA's convergence speed is much higher and better than the GA and ABSO. Yang et al. [52] reported that the multi-objective firefly algorithm achieves the best result in the 200th iteration (1000 iterations in total). Cao and Ye [53] also showed that the best Coarse-Grained Parallel Genetic Algorithm performance is approximately achieved in the 800th iteration when there are 1000 iterations. Amaireh et al. [54] also reported that the Antlion optimization algorithm starts converging to optimum value at almost 300 iterations (1000 iterations in total).

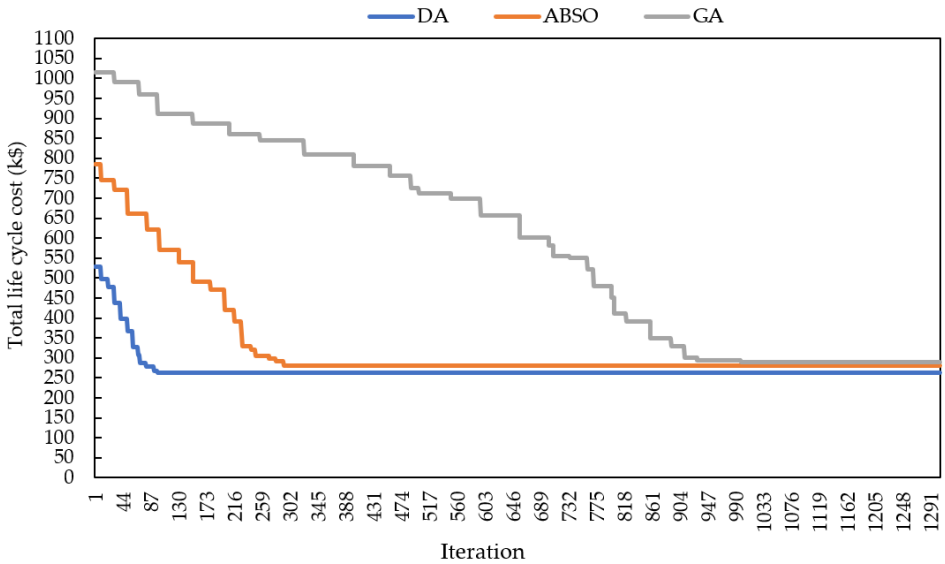

Figure 9. Convergence speed of the DA, GA, and ABSO optimization algorithms.

4. Conclusions and Further Works

Developing economic growth and social welfare depends on energy, especially electricity. However, electricity is usually generated by fossil fuels, whose adverse effects on the environment are well known. Accordingly, safe and clean electricity generation by renewable energy resources has currently been considered. The wind is one of the renewable

resources that its conversion to electricity is presently a matured technology. However, there is a time mismatch between power generation and consumption in systems based on renewable energy resources that could be solved using support units such as battery banks. Due to the significant cost and the high consumption of non-renewable energy in the production of system components, it should not overlook energy consumption and the costs of producing the system components. To have a reliable, low CExD, and cost-effective system, this paper optimizes the components' size of a desalination system integrated into a wind turbine plant to supply the freshwater of inhabitants of Larak Island, Iran by DA. Overall, results show the convergence speed to reach the optimal solution for the DA optimization algorithms than the GA and ABSO algorithms.

More specifically, the results showed that when LPSP is 10%, compared to when LPSP is 0%, the total CExD and total LCC are reduced by 34.76% when the battery is full and 45.44% when the battery is empty and there is a 44.43% decrease in the total LLC, respectively. Moreover, based on the results, exergy removal from nature in freshwater production by developed configuration is primarily in the form of "renewable, kinetic" in the range of 5.56–9.46 MJ/FU and followed by "non-renewable, fossil" in the range of 1.8–2.17 MJ/FU when the battery is full. Due to the consumption of wind energy to charge the batteries, the share of this energy increased compared to when the batteries are fully charged. The water tank and battery exhibited the highest effect on the "non-renewable, fossil" impact category, for all different LPSP (%). The bio-polyethylene application instead of fossil-polyethylene production in water tank production and the application of metal oxides instead of graphite in battery production are promising approaches for reducing fossil fuel consumption. Although the more reliable the system has a higher CExD, the system with higher reliability lead to less exergy loss during the production of 1 m^3 freshwater by SWROD/WT/BBS. It should be noted that the main limitation of the proposed solution here is that in the real world, there are cases that may affect the energy consumption of the desalination plant that is not considered in this solution. A database has also been used to analyze the exergy, and the exergy flow may be slightly different in the real world and the target area.

Future studies should also pursue these objective functions for desalination integrated to other renewable energy resources such as solar energy, geothermal energy, biomass, etc.

Author Contributions: Conceptualization, M.K., A.M. and H.H.-B.; methodology, M.K.; software, M.K.; validation, M.K.; formal analysis, M.K., A.M. and H.H.-B.; investigation, M.K.; resources, M.K.; data curation, M.K.; writing—Original draft preparation, M.K.; writing—Review and editing, A.M. and H.H.-B.; supervision, A.M.; project administration, A.M.; funding acquisition, A.M. All authors have read and agreed to the published version of the manuscript.

Funding: This research received no external funding.

Institutional Review Board Statement: Not applicable.

Informed Consent Statement: Not applicable.

Data Availability Statement: The data presented in this study are available in insert article.

Conflicts of Interest: The authors declare no conflict of interest.

Nomenclature

A_{WT}	Total area swept by the WT generator blades (m^2)
Ca_{WD}	Capacity of SWRO desalination system (m^3/day)
C_{BBS}	Battery bank cost ($)
CC	Capital cost ($)
C_{CH}	Cost of chemicals ($/$m^3$)
$C_{Conv/Inv}$	Converter/inverter price ($)
C_{DP}	Cumulative degree of perfection
CED	Cumulative energy demand

CExD	Cumulative exergy demand
$C_{Mnt\text{-}BBS}$	Annual maintenance cost of the battery ($/year)
$C_{Mnt\text{-}Conv/Inv}$	Annual maintenance cost of converter/inverter ($/year)
$C_{Mnt\text{-}SWROD}$	Maintenance cost of SWROD system ($/m^3)
$C_{Mnt\text{-}WT}$	Annual maintenance costs of wind turbine ($/year)
C_{MR}	membrane replacement cost ($/m^3)
CP	Wind power coefficient
CRF	Capital recovery factor
C_{SWROD}	Cost of SWROD unit per m^3/day ($/m^3/day)
C_{WT}	Wind turbine price ($)
C_{WTa}	Water tank cost ($/m^3)
DA	Division algorithm
DOD	Maximum depth of discharge (%)
DWD	Daily freshwater demand (m^3/day)
EIA	Energy information administration
GA	Genetic algorithm
GHG	Greenhouse gases
H_{WD}	Hourly water demand (m^3/h)
i	Interest rate (%)
LPSP	Loss of power supply probability (%)
$LPSP^m$	Maximum allowable LPSP (%)
MC	Maintenance cost ($)
n	Project lifetime (year)
N_{BBS}	Number of batteries
η_{bc}	Charge efficiency of the battery bank (%)
η_{bf}	Discharging efficiency of the battery bank (%)
η_{Inv}	Converter/inverter efficiency (%)
N_{Me}	Number of membrane replacements per year
N_{WT}	Number of wind turbine
η_{WT}	Wind turbine reference efficiency (%)
P_D	Desalination installed power (kW)
P_{DEM}	Power consumption of SWROD plant (kW)
P_{DI}	Nominal load of the SWROD plant (kW)
P_{Inv}	Nominal converter/inverter power (kW)
P_L	Annual load demand (kW)
P_{MD}	Minimum load of the SWROD plant (kW)
P_r	Rated power of the wind turbine (kW)
PW_{BBS}	Factor of payment present worth of battery
$PW_{Conv/Inv}$	Factor of payment present worth of Conv/Inv
P_{WT}	Output power of wind turbine (kW)
S_{BBS}	Nominal capacity of battery bank (kWh)
S_{DC}	Specific energy consumption (kWh/m^3)
SOC(t)	State of the battery charge at the time t (kWh)
SOC(t−1)	State of the battery charge at the time t−1(kWh)
SOC_{max}	Maximum charge of the battery bank (kWh)
SOC_{min}	Minimum charge of the battery bank (kWh)
TC_{CH}	Cost of chemicals of ROD unit ($)
TC_{MR}	Membrane replacement cost of ROD unit ($)
TLCC	Total life cycle cost ($)
V_{ci}	Cut-in wind speed (m/s)
V_{co}	Cut-out wind speed (m/s)
V_r	Nominal wind speed (m/s)
V_{WTa}	Fresh water tank volumetric capacity (m^3)
η_{PC}	Power conditioning efficiency (%)
η_r	Reducer efficiency (%)
ρ_a	Air density (kg/m^3)
σ	Hourly self-discharge rate (%)

References

1. Ahmed, F.E.; Hashaikeh, R.; Diabat, A.; Hilal, N. Mathematical and optimization modelling in desalination: State-of-the-art and future direction. *Desalination* **2019**, *469*, 114092. [CrossRef]
2. Abid, A.; Jamil, M.A.; us Sabah, N.; Farooq, M.U.; Yaqoob, H.; Khan, L.A.; Shahzad, M.W. Exergoeconomic optimization of a forward feed multi-effect desalination system with and without energy recovery. *Desalination* **2021**, *499*, 114808. [CrossRef]
3. Behzadi, A.; Habibollahzade, A.; Zare, V.; Ashjaee, M. Multi-objective optimization of a hybrid biomass-based SOFC/GT/double effect absorption chiller/RO desalination system with CO2 recycle. *Energy Convers. Manag.* **2019**, *181*, 302–318. [CrossRef]
4. Abdelshafy, A.M.; Hassan, H.; Jurasz, J. Optimal design of a grid-connected desalination plant powered by renewable energy resources using a hybrid PSO-GWO approach. *Energy Convers. Manag.* **2018**, *173*, 331–347. [CrossRef]
5. Ali, A.; Tufa, R.A.; Macedonio, F.; Curcio, E.; Drioli, E. Membrane technology in renewable-energy-driven desalination. *Renew. Sustain. Energy Rev.* **2018**, *81*, 1–21. [CrossRef]
6. Mehrjerdi, H. Modeling, integration, and optimal selection of the turbine technology in the hybrid wind-photovoltaic renewable energy system design. *Energy Convers. Manag.* **2020**, *205*, 112350. [CrossRef]
7. Tito, S.R.; Lie, T.T.; Anderson, T.N. Optimal sizing of a wind-photovoltaic-battery hybrid renewable energy system considering socio-demographic factors. *Sol. Energy* **2016**, *136*, 525–532. [CrossRef]
8. McManus, M.C. Environmental consequences of the use of batteries in low carbon systems: The impact of battery production. *Appl. Energy* **2012**, *93*, 288–295. [CrossRef]
9. Bahlawan, H.; Poganietz, W.-R.; Spina, P.R.; Venturini, M. Cradle-to-gate life cycle assessment of energy systems for residential applications by accounting for scaling effects. *Appl. Therm. Eng.* **2020**, *171*, 115062. [CrossRef]
10. Alvarenga, R.A.F.; de Oliveira Lins, I.; de Almeida Neto, J.A. Evaluation of abiotic resource LCIA methods. *Resources* **2016**, *5*, 13. [CrossRef]
11. Valderrama, C.; Granados, R.; Cortina, J.L.; Gasol, C.M.; Guillem, M.; Josa, A. Implementation of best available techniques in cement manufacturing: A life-cycle assessment study. *J. Clean. Prod.* **2012**, *25*, 60–67. [CrossRef]
12. Behrooznia, L.; Sharifi, M.; Alimardani, R.; Mousavi-Avval, S.H. Sustainability analysis of landfilling and composting-landfilling for municipal solid waste management in the north of Iran. *J. Clean. Prod.* **2018**. [CrossRef]
13. Bösch, M.E.; Hellweg, S.; Huijbregts, M.A.J.; Frischknecht, R. Applying cumulative exergy demand (CExD) indicators to the ecoinvent database. *Int. J. Life Cycle Assess.* **2007**, *12*, 181. [CrossRef]
14. Iskin, I.; Taha, R.A.; Daim, T.U. Exploring the adoption of alternative energy technologies: A literature review. *Int. J. Sustain. Soc.* **2013**, *5*, 43–61. [CrossRef]
15. Irfan, M.; Hao, Y.; Ikram, M.; Wu, H.; Akram, R.; Rauf, A. Assessment of the public acceptance and utilization of renewable energy in Pakistan. *Sustain. Prod. Consum.* **2021**, *27*, 312–324. [CrossRef]
16. Ekhteraei Toosi, H.; Merabet, A.; Swingler, A. Dual layer power scheduling strategy for EV ESS controllable load in bi directional dynamic markets for low cost implementation. *Int. Trans. Electr. Energy Syst.* **2021**, *31*, e12681. [CrossRef]
17. Zhao, G.; Nielsen, E.R.; Troncoso, E.; Hyde, K.; Romeo, J.S.; Diderich, M. Life cycle cost analysis: A case study of hydrogen energy application on the Orkney Islands. *Int. J. Hydrog. Energy* **2019**, *44*, 9517–9528. [CrossRef]
18. Zhang, W.; Maleki, A.; Rosen, M.A.; Liu, J. Optimization with a simulated annealing algorithm of a hybrid system for renewable energy including battery and hydrogen storage. *Energy* **2018**, *163*, 191–207. [CrossRef]
19. Mayer, M.J.; Szilágyi, A.; Gróf, G. Environmental and economic multi-objective optimization of a household level hybrid renewable energy system by genetic algorithm. *Appl. Energy* **2020**, *269*, 115058. [CrossRef]
20. Rathish, R.J.; Mahadevan, K.; Selvaraj, S.K.; Booma, J. Multi-objective evolutionary optimization with genetic algorithm for the design of off-grid PV-wind-battery-diesel system. *Soft Comput.* **2021**, *25*, 3175–3194. [CrossRef]
21. Pillai, A.C.; Thies, P.R.; Johanning, L. Development of a Multi-Objective Genetic Algorithm for the Design of Offshore Renewable Energy Systems. In Proceedings of the World Congress of Structural and Multidisciplinary Optimisation, Braunschweig, Germany, 5–9 June 2017; pp. 2013–2026.
22. Saiprasad, N.; Kalam, A.; Zayegh, A. Triple bottom line analysis and optimum sizing of renewable energy using improved hybrid optimization employing the genetic algorithm: A case study from India. *Energies* **2019**, *12*, 349. [CrossRef]
23. Starke, A.R.; Cardemil, J.M.; Escobar, R.; Colle, S. Multi-objective optimization of hybrid CSP+ PV system using genetic algorithm. *Energy* **2018**, *147*, 490–503. [CrossRef]
24. Wang, Y.; Wei, C. Design optimization of office building envelope based on quantum genetic algorithm for energy conservation. *J. Build. Eng.* **2021**, *35*, 102048. [CrossRef]
25. Su, Y.; Guo, N.; Tian, Y.; Zhang, X. A non-revisiting genetic algorithm based on a novel binary space partition tree. *Inf. Sci.* **2020**, *512*, 661–674. [CrossRef]
26. Kiehbadroudinezhad, M.; Rajabipour, A.; Cada, M.; Khanali, M. Modeling, design, and optimization of a cost effective and reliable hybrid renewable energy system integrated with desalination using the division algorithm. *Int. J. Energy Res.* **2021**, *45*, 429–452. [CrossRef]
27. Manju, S.; Sagar, N. Renewable energy integrated desalination: A sustainable solution to overcome future fresh-water scarcity in India. *Renew. Sustain. Energy Rev.* **2017**, *73*, 594–609. [CrossRef]
28. Ardjal, A.; Merabet, A.; Bettayeb, M.; Mansouri, R.; Labib, L. Design and implementation of a fractional nonlinear synergetic controller for generator and grid converters of wind energy conversion system. *Energy* **2019**, *186*, 115861. [CrossRef]

29. Li, R.; Guo, S.; Yang, Y.; Liu, D. Optimal sizing of wind/concentrated solar plant/electric heater hybrid renewable energy system based on two-stage stochastic programming. *Energy* **2020**, *209*, 118472. [CrossRef]
30. Tanvir, A.A.; Merabet, A. Artificial neural network and Kalman filter for estimation and control in standalone induction generator wind energy DC microgrid. *Energies* **2020**, *13*, 1743. [CrossRef]
31. Balat, M. A review of modern wind turbine technology. *Energy Sources A* **2009**, *31*, 1561–1572. [CrossRef]
32. Gan, L.K.; Shek, J.K.H.; Mueller, M.A. Hybrid wind-photovoltaic-diesel-battery system sizing tool development using empirical approach, life-cycle cost and performance analysis: A case study in Scotland. *Energy Convers. Manag.* **2015**, *106*, 479–494. [CrossRef]
33. Spyrou, I.D.; Anagnostopoulos, J.S. Design study of a stand-alone desalination system powered by renewable energy sources and a pumped storage unit. *Desalination* **2010**, *257*, 137–149. [CrossRef]
34. Wu, B.; Maleki, A.; Pourfayaz, F.; Rosen, M.A. Optimal design of stand-alone reverse osmosis desalination driven by a photovoltaic and diesel generator hybrid system. *Sol. Energy* **2018**, *163*, 91–103. [CrossRef]
35. Szargut, J. Exergy analysis. *Mag. Polish Acad. Sci.* **2005**, *3*, 31–33.
36. Sun, B.; Nie, Z.; Gao, F.; Liu, Y.; Wang, Z.; Gong, X. Cumulative exergy demand analysis of the primary aluminum produced in China and its natural resource-saving potential in transportation. *Int. J. Life Cycle Assess.* **2015**, *20*, 1048–1060. [CrossRef]
37. Wernet, G.; Bauer, C.; Steubing, B.; Reinhard, J.; Moreno-Ruiz, E.; Weidema, B. The ecoinvent database version 3 (part I): Overview and methodology. *Int. J. Life Cycle Assess.* **2016**, *21*, 1218–1230. [CrossRef]
38. Amiri, Z.; Asgharipour, M.R.; Campbell, D.E.; Armin, M. Extended exergy analysis (EAA) of two canola farming systems in Khorramabad, Iran. *Agric. Syst.* **2020**, *180*, 102789. [CrossRef]
39. Zhang, G.; Wu, B.; Maleki, A.; Zhang, W. Simulated annealing-chaotic search algorithm based optimization of reverse osmosis hybrid desalination system driven by wind and solar energies. *Sol. Energy* **2018**, *173*, 964–975. [CrossRef]
40. Maleki, A.; Pourfayaz, F.; Ahmadi, M.H. Design of a cost-effective wind/photovoltaic/hydrogen energy system for supplying a desalination unit by a heuristic approach. *Sol. Energy* **2016**, *139*, 666–675. [CrossRef]
41. Maleki, A.; Khajeh, M.G.; Rosen, M.A. Weather forecasting for optimization of a hybrid solar-wind-powered reverse osmosis water desalination system using a novel optimizer approach. *Energy* **2016**, *114*, 1120–1134. [CrossRef]
42. Gaur, S.; Chahar, B.R.; Graillot, D. Analytic elements method and particle swarm optimization based simulation-optimization model for groundwater management. *J. Hydrol.* **2011**, *402*, 217–227. [CrossRef]
43. Kiehbadroudinezhad, S.; Bousquet, J.-F.; Cada, M.; Short, C.I.; Shahabi, A.; Kiehbadroudinezhad, S. Expansion of a Y-Shaped Antenna Array and Optimization of the Future Antenna Array in Malaysia for Astronomical Applications. *J. Mod. Phys.* **2019**, *10*, 888–908. [CrossRef]
44. Benavides, P.T.; Lee, U.; Zarè-Mehrjerdi, O. Life cycle greenhouse gas emissions and energy use of polylactic acid, bio-derived polyethylene, and fossil-derived polyethylene. *J. Clean. Prod.* **2020**, *277*, 124010. [CrossRef]
45. Tian, S.; Tang, H.; Wang, Q.; Yuan, X.; Ma, Q.; Wang, M. Evaluation and optimization of blanket production from recycled polyethylene terephthalate based on the coordination of environment, economy, and society. *Sci. Total Environ.* **2021**, *772*, 145049. [CrossRef] [PubMed]
46. Spierling, S.; Venkatachalam, V.; Mudersbach, M.; Becker, N.; Herrmann, C.; Endres, H.-J. End-of-life options for bio-based plastics in a circular economy-status quo and potential from a life cycle assessment perspective. *Resources* **2020**, *9*, 90. [CrossRef]
47. Spierling, S.; Röttger, C.; Venkatachalam, V.; Mudersbach, M.; Herrmann, C.; Endres, H.-J. Bio-based plastics-A building block for the circular economy? *Procedia CIRP* **2018**, *69*, 573–578. [CrossRef]
48. Rahman, M.H.; Bhoi, P.R. An overview of non-biodegradable bioplastics. *J. Clean. Prod.* **2021**, *294*, 126218. [CrossRef]
49. Notter, D.A.; Gauch, M.; Widmer, R.; Wager, P.; Stamp, A.; Zah, R.; Althaus, H.-J. Contribution of Li-ion batteries to the environmental impact of electric vehicles. *Environ. Sci. Technol.* **2010**, *44*, 6550–6556. [CrossRef] [PubMed]
50. Padashbarmchi, Z.; Hamidian, A.H.; Khorasani, N.; Kazemzad, M.; McCabe, A.; Halog, A. Environmental life cycle assessments of emerging anode materials for Li ion batteries metal oxide NP s. *Environ. Prog. Sustain. Energy* **2015**, *34*, 1740–1747. [CrossRef]
51. Nikkhah, A.; Kosari-Moghaddam, A.; Troujeni, M.E.; Bacenetti, J.; Van Haute, S. Exergy flow of rice production system in Italy: Comparison among nine different varieties. *Sci. Total Environ.* **2021**, *781*, 146718. [CrossRef]
52. Yang, X.-S. Multiobjective firefly algorithm for continuous optimization. *Eng. Comput.* **2013**, *29*, 175–184. [CrossRef]
53. Cao, K.; Ye, X. Coarse-grained parallel genetic algorithm applied to a vector based land use allocation optimization problem: The case study of Tongzhou Newtown, Beijing, China. *Stoch. Environ. Res. Risk Assess.* **2013**, *27*, 1133–1142. [CrossRef]
54. Amaireh, A.A.; Alzoubi, A.; Dib, N.I. Design of linear antenna arrays using antlion and grasshopper optimization algorithms. In Proceedings of the 2017 IEEE Jordan Conference on Applied Electrical Engineering and Computing Technologies (AEECT), Aqaba, Jordan, 11–13 October 2017; pp. 1–6.